Theor Chem Acc (2011) 128:541–553
DOI 10.1007/s00214-010-0830-7

REGULAR ARTICLE

Theoretical evaluation of the nature and strength of the F···F intermolecular interactions present in fluorinated hydrocarbons

Reyes Malavé Osuna · Victor Hernández · Juan T. López Navarrete · Emiliana D'Oria · Juan J. Novoa

Received: 9 July 2010 / Accepted: 18 September 2010 / Published online: 8 October 2010

Abstract The nature, strength and directionality of C–F···F interactions were theoretically evaluated on all symmetry unique dimers present in the CF_4, C_2F_4 and C_6F_6 crystals and on CF_4, CHF_3, CH_2F_2 and CH_3F model dimers placed in two different geometries. On each dimer, the interaction energy was computed at the MP2/aug-cc-pVDZ level, and also an Atoms in Molecule analysis of the dimer electron density was done to find all intermolecular bonds. The characterization was completed by computing the energy components of the dimer interaction energy, using the SAPT method. The results show that in most dimers found in the CF_4, C_2F_4 and C_6F_6 crystals, there are more than one C–F···F intermolecular bond and sometimes even a C–F···π intermolecular bond. By selecting dimers presenting one C–F···F bond, the following strength can be estimated for a single C–F···F bond: −0.21 kcal/mol in C(sp^3) atoms, −0.25 kcal/mol in C(non-aromatic sp^2), −0.41 kcal/mol in C(aromatic sp^2). The interaction energy of the dimer grows almost linearly with the number of C–F···F bonds present. The relative orientation of the C–F···F bond affects the bond strength. The SAPT calculations indicate that in collinear dimers, C–F···F interactions are strongly dominated by the dispersion energetic component, while when in non-collinear conformations the electrostatic component can be as important as the dispersion one.

Keywords C–F···F intermolecular interactions · MP2 · CCSD(T) · AIM · SAPT calculations · CF_4 · C_2F_4 · C_6F_6 · CHF_3 · CH_2F_2 · CH_3F

1 Introduction

The interest in producing bipolar transistors and other circuits has recently increased the interest on the structure of perfluoroacene crystals [1]. Producing bipolar transistors requires a p-type carrier and molecule with similar physical and electrical properties, but with n-type of carriers. Pentacene is a largely studied prototypical example, due to its electronic transport properties in thin films [2] and p-type semiconductor behaviour [3]. At the same time, perfluoroacences have long been recognized as a potential counterpart to pentacene in bipolar transistors, because the perfluorination of pentacene transforms a good p-type organic semiconductor in an efficient n-type one [4], and the electrical properties of perfluoroacences depend on their crystal packing. Experimental studies have shown that although perfluorination in aromatic polyacenes induces important changes in the electronic and charge-transport properties compared with those of their parent compounds, the crystal packing of the perfluorinated and hydrogenated solids is very similar [5]. However, the reasons for such similarity are not fully understood. This fact prompted us

Published as part of the special issue celebrating theoretical and computational chemistry in Spain.

Electronic supplementary material The online version of this article (doi:10.1007/s00214-010-0830-7) contains supplementary material, which is available to authorized users.

R. M. Osuna · V. Hernández · J. T. L. Navarrete
Departamento Química-Física, Universidad de Málaga, 29071 Málaga, Spain

E. D'Oria (✉) · J. J. Novoa (✉)
Departamento Química-Física and IQTCUB, Facultat de Química, Universitat de Barcelona, Av. Diagonal 647, 08028 Barcelona, Spain
e-mail: e.doria@ub.edu

J. J. Novoa
e-mail: juan.novoa@ub.edu

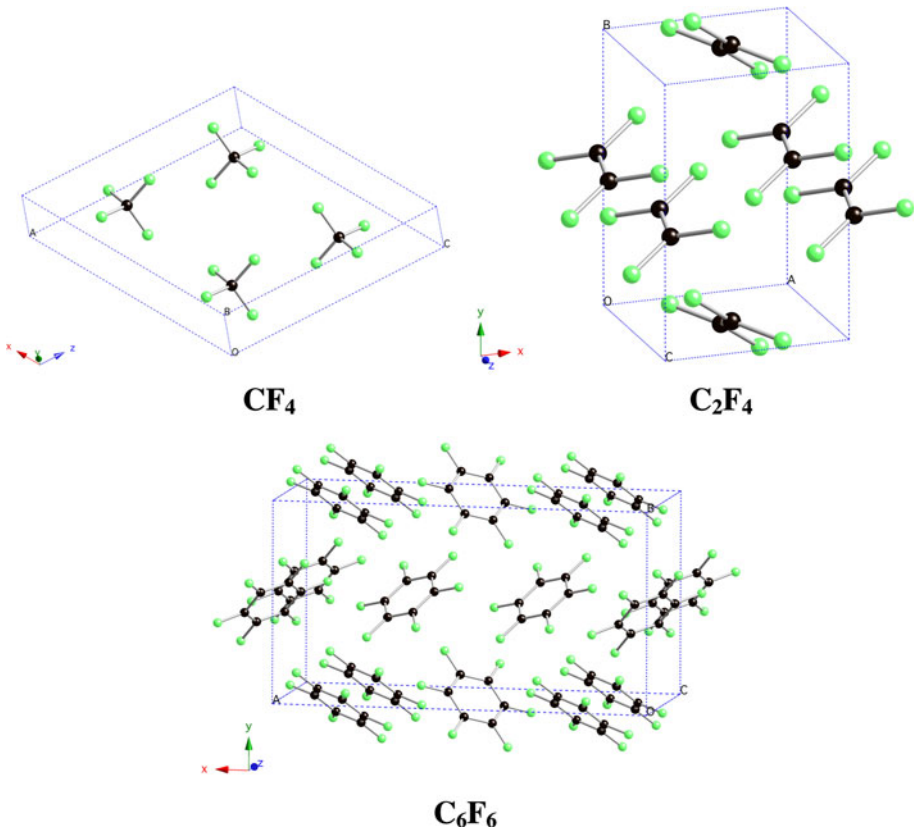

Fig. 1 Structure of the CF_4, C_2F_4 and C_6F_6 crystals

to perform an in-depth theoretical study of the crystal packing of perfluorinated molecular solids, which started by the study of the C–F···F interactions in the CF_4, C_2F_4 and C_6F_6 crystals (their structure is shown in Fig. 1), taken as prototype examples for the study of C(sp^3)–F···F, C(non-aromatic-sp^2)–F···F and C(aromatic-sp^2)–F···F interactions.

There are other fluorinated compounds where C–F···F interactions are also relevant. Among them are fluorinated alkenes, important starting materials in the polymer industry [6]. Other examples are found in the pharmaceutical industry, where fluorinated hydrocarbons are used in some drugs due to the similar biological activity of F-substituted compounds and their hydrogenated analogues, being the former more resistant to metabolic degradation. However, as not every crystal presenting C–F···F interactions is necessarily perfluorinated, we widened our study by comparing the strength and directionality of C–F···F interactions in CF_4 dimers with that found in CHF_3, CH_2F_2 and CH_3F dimers, helpful to understand C–F···F interactions in fully or partially F-substituted methyl groups.

Previous studies on C–F···F interactions, sometimes called organic fluorine, are controversial. C–F···F interactions are well covered in Hulliger and coworkers' review on organic fluorine (C–F groups) [7]. Some authors considered that F···F interactions are the only non-attractive halogen···halogen interaction and that they are just a consequence of other dominant features of the crystal packing [8]. Other authors, however, concluded that organic fluorine was an important tool in the crystal engineering of pharmaceutical compounds [9], particularly in the absence of strong intermolecular interactions. In fact, the analysis of the crystal packing of some drugs showed a significant role of weak interactions, including the F···F interactions [10], although the same study pointed out that the presence of short F···F interactions could be due to stronger intermolecular interactions (O–H···N) and suggested a charge density analysis to clarify this point. Alkorta et al. [11], combining NMR studies and an Atoms in Molecules (AIM) analysis [12], concluded that the density and Laplacian at the bond critical point associated with the F···F contacts are similar to those found in ionic bonds and hydrogen bonds. However, the nature of F···F interactions is still a subject of discussion, partly because they are found in competition with other interactions, as C–F···π or C–H···F [13] interactions, and not always the relative importance of each contribution is clear. This is where perflouro hydrocarbons are useful, as their crystals cannot present C–H···F interactions, although they still can present C–F···π interactions, in some cases. Therefore, the optimum solution to the problem is the use of advanced theoretical tools designed to establish when and where intermolecular bonds are formed,

as these available in the AIM methodology. The need of deeper theoretical analysis was already pointed out in recent analysis of the experimental evidence for the presence of F···F interactions [14].

Therefore, in order to improve the current understanding concerning the nature and properties on the C–F···F interactions, in this work, we will perform an in depth theoretical study of these interactions in three perfluoro hydrocarbon crystals, CF_4, C_2F_4 and C_6F_6, taken as prototype examples for the study of C(sp^3)–F···F, C(non-aromatic-sp^2)–F···F and C(aromatic-sp^2)–F···F interactions. The interaction energy and bond critical points in all symmetry unique dimers present in these crystals will be computed. Furthermore, the components of the interaction energy will be computed to establish on quantitative grounds the nature of their C–F···F interactions. Finally, the properties of the C–F···F interactions in CF_4···CF_4 dimers will be compared with those of CHF_3···CHF_3, CH_2F_2···CH_2F_2, and CH_3F···CH_3F dimers, prototypes of C–F···F interactions between perfluorinated methyl groups, in the first dimer, and of lower fluorinated hydrocarbons, in the latter two dimers.

2 Methodology

A possible way of getting complete information on the nature, strength and directionality of an intermolecular interaction is by taking a model dimer and looking at its properties at assumed relative positions of the dimer, wide enough as to cover all likely relative orientations of the dimer in their crystals. Alternatively, one can pick all symmetry unique dimers from the crystals of interest, as these are already the most likely relative orientations of the dimer in the crystals of interest, in this case, CF_4, C_2F_4 and C_6F_6, the smallest examples of perfluorinated hydrocarbons presenting respectively C(sp^3)–F···F, C(non-aromatic-sp^2)–F···F and C(aromatic-sp^2)–F···F interactions. The latter is the approach followed in this work.

On each of the selected dimers, the properties of their C–F···F intermolecular interactions were evaluated by performing the following three consecutive steps. First of all, the interaction energy of each dimer was computed using the Gaussian-03 package [15]. In each dimer, its interaction energy was obtained by subtracting the second-order Møller–Plesset (MP2) energy of the sum of the MP2 energy of the two isolated monomers. The basis set superposition error (BSSE) was corrected using the counterpoise method [16–18].[1,2] The accuracy of MP2 calculations was tested in one symmetry unique dimers of the CF_4 crystal by doing CCSD(T) calculations. Similarly, the basis set used in all dimers of this study was the aug-cc-pVDZ basis [19], a basis set of double zeta plus polarization quality that also includes diffuse functions on all atoms, selecting after extensive numerical test on the CF_4 dimer.

The second step in each dimer was the evaluation of the number and type of intermolecular (3,−1) bond critical points (BCPs), using the PROAIM program [20]. This determination allows a proper rationalization of the dimer interaction energy, based on the number of C–F···F bonds present and its competition or not with other intermolecular bonds. The properties of all BCPs were characterized by calculating the density and Laplacian at the BCP (ρ_{BCP} and ∇^2_{BCP}, respectively).

One can go one step forward and define on quantitative grounds the nature of the intermolecular C–F···F interaction in dimers where this is the only type of intermolecular bond present. This was the third step in our study. The interaction energy components were evaluated by SAPT computations [21] using the SAPT2008 program [22]. According to the SAPT method, the total interaction energy of a dimer can be perturbatively decomposed as the sum of the electrostatic (E_{el}), exchange (E_{ex}), induction (E_{ind}) and dispersion (E_{disp}) components:

$$E_{tot} = E_{el} + E_{ex} + E_{ind} + E_{disp} \quad (1)$$

where each of these terms was obtained from the energy components printed by the SAPT2008 program according to the following expressions:

$$E_{el} = E_{el}^{(10)} + E_{el,resp}^{(12)} \quad (2)$$

$$E_{ex} = E_{ex}^{(10)} + \varepsilon_{ex}^{(1)}(2) \quad (3)$$

$$E_{disp} = E_{disp}^{(20)} + E_{ex\text{-}disp}^{(20)} \quad (4)$$

$$E_{ind} = E_{ind,resp}^{(20)} + E_{ex\text{-}ind,resp}^{(20)} + \delta E_{ind,resp}^{HF} + {}^{t}E_{ind}^{(22)} + {}^{t}E_{ex\text{-}ind}^{(22)} \quad (5)$$

The physical meaning of these terms is the following: E_{el} at large distance is the electrostatic energy of monomers with the unperturbed electron distributions (at short distance also includes charge overlap and penetration effects), E_{ex} is meant to represent the electron repulsion energy due to the Pauli exclusion principle, E_{ind} is physically interpreted as the energy gain resulting from the induction interaction and includes the higher-order induction and exchange corrections, $\delta E^{HF}_{ind,\ resp}$, and, finally, E_{disp} is a non-classical term, which can be approximated visualized as resulting form the instantaneous interactions among the electrons.

The whole study was done first on all symmetry unique dimers found in the CF_4, C_2F_4 and C_6F_6 crystals. Then, on

[1] The validity of the counterpoise correction was analytically demonstrated in [17].

[2] A numerical demonstration of the validity of the counterpoise correction was shown in [18].

two specific orientations where only one C–F···F intermolecular bond was present, the strength of the CF_4···CF_4 dimer was compared against those of CHF_3···CHF_3, CH_2F_2···CH_2F_2 and CH_3F···CH_3F dimers, which allows to evaluate the properties of C–F···F interactions between fully perfluorinated methyl groups, in the first dimer, and of lower fluorinated hydrocarbons, in the latter two dimers.

3 Results and discussion

3.1 Assessment of the theoretical methodology to compute C–F···F interactions in crystals of perfluorinated hydrocarbons

Lone pair interactions are usually described as originating from the dispersion component. Therefore, given the large number of lone-electron pairs located on the two F atoms, the attractive part of C–F···F intermolecular interactions in CF_4, C_2F_4 or C_6F_6 dimers is expected to be dominated by the dispersion component. This suggests the use of the MP2 method for a proper evaluation of the interaction energy of CF_4···CF_4 and all other dimers of interest here, as the MP2 method is known to account for a large amount of dispersion component. In any case, the quality of the MP2 method interaction energy of perfluoro hydrocarbon dimers will be confirmed below by comparing its results with those obtained from CCSD(T) calculations.

Table 1 collects the Hartree-Fock (HF) and MP2 interaction energy (BSSE corrected an uncorrected) computed using various basis sets of increasing quality that range from the 6-31G to the correlation consistent aug-cc-pVQZ basis set. They were obtained for dimer B of the CF_4 crystal, which as we will see later on, presents only one C–F···F intermolecular bond. All BSSE-corrected HF interaction energies are repulsive, while all BSSE-corrected MP2 values are attractive, a fact that confirms the previous expectations on the relevance for the stability of this dimer of the dispersion interactions. The BSSE-corrected interaction energy computed with the largest basis set (−0.27 kcal/mol, aug-ccpVQZ results) is just 0.01 kcal/mol lower than that obtained with the aug-cc-pVTZ basis set, and 0.06 kcal/mol lower than that got with the aug-cc-pVDZ. These results show the smooth convergence of the MP2/aug-cc-pVXZ interaction energy, which is practically converged when using the aug-cc-pVQZ, basis. They also suggest that a good cost/quality basis for the remaining computations is the aug-cc-pVDZ, which was chosen for all remaining calculations done in this work. It is also worth pointing the much smaller convergence ratio of the cc-pVXZ basis sets and of the 6-31G basis. It is also evident that correcting the BSSE is crucial to get non-erratic values for the interaction energy.

Using the aug-cc-pVDZ basis set, a test on the quality of the MP2 results was done by comparing the MP2 and CCSD(T) results on CF_4···CF_4 dimer B (that also used in Table 1). The results, shown in Table 2, indicate that the BSSE-corrected CCSD(T) interaction energy is just 0.04 kcal/mol more stable than the MP2 result. This confirms the accuracy of the MP2 results.

Table 2 Intermolecular energy computed for CF_4 dimer B using the aug-cc-pVDZ and the indicated method

Method	ΔE/kcal/mol
MP2	−0.21
MP3	−0.19
MP4(DQ)	−0.17
MP4(SDQ)	−0.20
CCSD(T)	−0.25

All the energies are corrected by counterpoise method

Table 1 Interaction energy for the CF_4 dimer B (see Fig. 2) calculated with the indicated basis set at the geometry of the dimer in the CF_4 crystal

Basis set name	# functions	HF_c (kcal/mol)	HF_{nc} (kcal/mol)	$MP2_c$ (kcal/mol)	$MP2_{nc}$ (kcal/mol)	BSSE MP2 (kcal/mol)
6-31G	90	0.19	−0.01	0.05	−0.22	−0.27
cc-pVDZ	140	0.14	−0.09	−0.05	−0.36	−0.31
6-31++G(d,p)	190	0.17	−0.01	−0.15	−0.73	−0.58
aug-cc-pVDZ	230	0.16	−0.09	−0.21	−0.71	−0.50
cc-pVTZ	300	0.16	0.06	−0.15	−0.34	−0.19
aug-cc-pVTZ	460	0.16	0.07	−0.26	−0.50	−0.24
cc-pVQZ	550	0.16	0.13	−0.21	−0.29	−0.08
aug-cc-pVQZ	800	0.16	0.12	−0.27	−0.39	−0.12

The total number of functions in the basis set is given in the second column. The calculation was done using the HF and MP2 methods, and the interaction energy was computed with and without counterpoise correction (respectively identified by the subindex c and nc). The value of the basis set superposition error (BSSE) of the MP2 calculation is included in the last column to facilitate comparisons

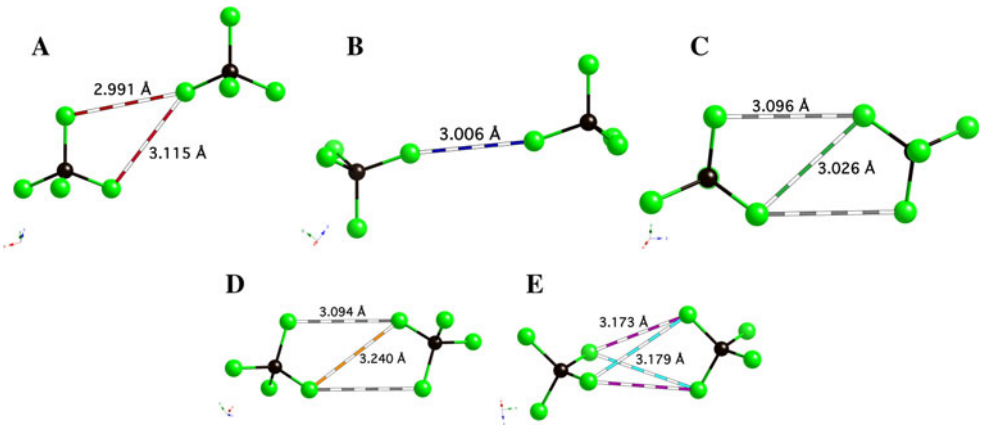

Fig. 2 Geometry of the five non-symmetry equivalent dimers present in the CF_4 crystal (Ref. [23] TFMETH02). The *broken lines* mark the F atoms involved in C–F···F intermolecular bonds

3.2 The nature of C–F···F interactions in crystals of perfluorinated hydrocarbons

Once the computational methodology employed in the evaluation of the C–F···F interaction energy has been assessed, we focussed our attention on evaluating the interaction energy for all symmetry unique dimers found in the three model perfluorinated crystals: CF_4, C_2F_4 and C_6F_6.

The CF_4 crystal (CCDB Ref. [23] TFMETH02) is the smallest perfluorinated hydrocarbon crystal and presents C(sp^3)–F···F interactions. The search of all symmetry unique dimers was done by looking at all the pairs having F···F contacts within the sum of van der Waals radii plus 0.2 Å (2.97 + 0.2 Å). Five unique pairs were found, whose geometry is shown in Fig. 2. The interaction energy of each of these pairs is collected in Table 3, together with the F···F distance for all C–F···F intermolecular bonds.

An AIM analysis of the MP2/aug-cc-pVDZ electronic density was also done on each dimer in order to locate all (3,−1) intermolecular bond critical points. This allowed establishing on solid basis the presence of all F···F intermolecular bonds (broken lines in Fig. 2) and their characteristics (see Table 3). No other type of intermolecular bond was detected.

All dimers in the CF_4 crystal have an attractive intermolecular interaction energy, being the strongest one −0.44 kcal/mol and the weakest one −0.21 kcal/mol. Two F···F (3,−1) bond critical points (BCP) were located in all dimers except dimer B, which showed only one (dimer B was that selected to carry out the assessment of the basis set and method). In all cases, the density at the bond critical point (ρ_{BCP}) was around 10^{-3} atomic units, and the Laplacian at the point ($\nabla^2\rho_{BCP}$) around 10^{-2} atomic units. These values are within the typical range found in ionic bonds and hydrogen bonds, in good agreement with the results from previous studies [11]. It is also worth pointing that when two BCPs are located between the fragments, the dimer intermolecular interaction is stronger (almost twice the interaction of dimer B, where only one BCP was found).

Table 3 BSSE-corrected intermolecular interaction energy calculated at MP2/aug-cc-pVDZ level of theory for each CF_4 dimer shown in Fig. 2

Dimer	F···F/Å	ΔE/kcal mol^{-1}	ρ_{BCP}/u.a.	$\nabla^2\rho_{BCP}$/u.a.
A	2.991	−0.30	4.06×10^{-3}	2.55×10^{-2}
	3.115		2.92×10^{-3}	2.02×10^{-2}
B	3.006	−0.21	3.21×10^{-3}	2.16×10^{-2}
C	3.026	−0.44	4.46×10^{-3}	2.74×10^{-2}
	3.096		3.34×10^{-3}	2.22×10^{-2}
	3.096		3.34×10^{-3}	2.22×10^{-2}
D	3.094	−0.35	3.25×10^{-3}	2.13×10^{-2}
	3.240		2.39×10^{-3}	1.75×10^{-2}
	3.240		2.39×10^{-3}	1.75×10^{-2}
E	3.173	−0.41	2.85×10^{-3}	1.96×10^{-2}
	3.173		2.85×10^{-3}	1.96×10^{-2}
	3.179		2.81×10^{-3}	1.94×10^{-2}
	3.179		2.81×10^{-3}	1.94×10^{-2}

For each dimer, the F···F contacts that present (3,−1) bond critical points are indicated. For each of them, the F···F distance, the density (ρ_{BCP}) and the Laplacian ($\nabla^2\rho_{BCP}$) are indicated, together with the BSSE-corrected interaction energy of the dimer (ΔE)

A similar crystal analysis about the dimers strength was done on the C_2F_4 crystal (Ref. [23] GAFLIJ, see Fig. 1), crystal that presents C(sp^2)–F···F interactions. Five non-symmetry–related C_2F_4···C_2F_4 dimers were located in this crystal (see Fig. 3). Their intermolecular interaction energy, also calculated at the MP2/aug-cc-pVDZ level, is collected in Table 4. Furthermore, on each dimer an AIM analysis of the MP2/aug-cc-pVDZ electronic density was also done in order to locate all (3,−1) intermolecular bond critical points. This allowed establishing on solid basis the presence of all F···F intermolecular bonds (broken lines in Fig. 3) and their characteristics (Table 4), along the presence of any other intermolecular bonds.

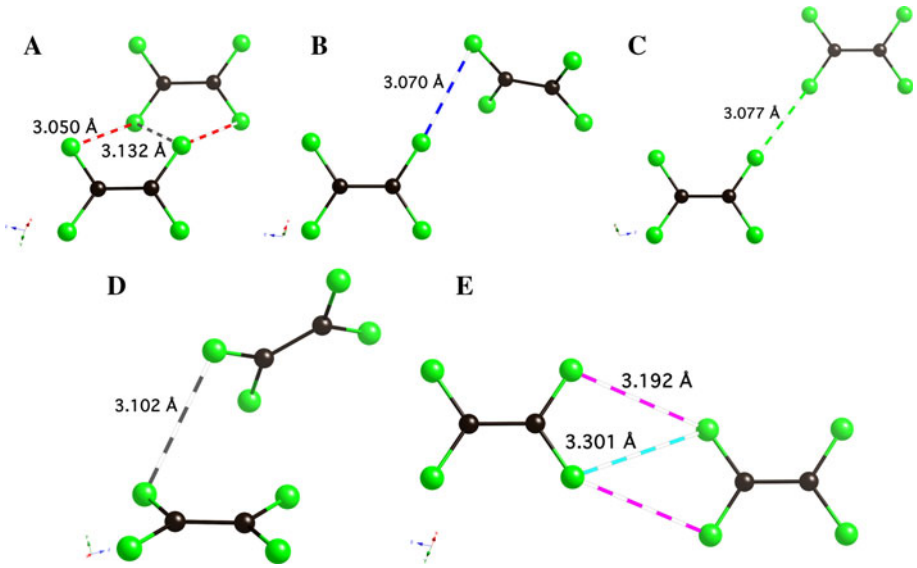

Fig. 3 Geometry of the five symmetry unique dimers found in the C_2F_4 crystal (Ref. [23] GAFLIJ). The *broken lines* mark the F atoms involved in C–F···F intermolecular bonds

Table 4 BSSE-corrected interaction energy calculated at MP2/aug-cc-pVDZ level for the five non-symmetry–related dimers found in the C_2F_4 crystals, shown in Fig. 3

Dimer	F···F/Å	ΔE/kcal mol^{-1}	ρ_{BCP}/u.a.	$\nabla^2\rho$/u.a.
A	3.050	−0.87	3.77×10^{-3}	2.42×10^{-2}
	3.050		3.77×10^{-3}	2.42×10^{-2}
	3.132		3.17×10^{-3}	2.21×10^{-2}
B	3.070	−0.72	10^{-4}	[a]
C	3.077	−0.25	2.68×10^{-3}	1.89×10^{-2}
D	3.102	−1.01	3.40×10^{-3}	2.26×10^{-2}
E	3.192	−0.42	2.46×10^{-3}	1.73×10^{-2}
	3.192		2.46×10^{-3}	1.73×10^{-2}
	3.301		1.96×10^{-3}	1.49×10^{-2}

The density (ρ_{BCP}) and the Laplacian ($\nabla^2\rho_{BCP}$) at the bond critical points are also given (Fig. 3 also shows, by means of broken lines, the F···F atoms linked by these bond critical point)

[a] Due to accuracy limitations of the PROAIM code, this point was graphically estimated (see Fig. S1). This procedure did not allow an estimation of $\nabla^2\rho_{BCP}$

A look at Table 4 shows that all dimers are energetically stable, with interaction energies within the range from −0.25 to −1.01 kcal/mol. The weakest interaction is found in dimer C, which presents only one F···F (3,−1) bond critical point and no other intermolecular bond. Thus, the interaction energy (−0.25 kcal/mol) can be taken as equal to the C–F···F strength for a C(sp^2) carbon. Therefore, C(sp^2)–F···F bonds in the C_2F_4 crystal are slightly stronger than the C(sp^3)–F···F bonds found in the CF_4 crystal (−0.21 kcal/mol, dimer B). These two results measure the impact of carbon hybridization in C–F···F interactions. Dimers B and D of C_2F_4 also present one F···F (3,−1) BCPs, but their interaction energy is a lot stronger, probably due to the presence of a C–F···π bond, manifested by the existence of a F···C (3,−1) BCP (see Fig. S2; typically $\rho_{BCP} = 4 \times 10^{-3}$ a.u. and $\nabla^2\rho = 2 \times 10^{-2}$ a.u.). Finally, dimers A and E of C_2F_4, all have two F···F (3,−1) BCPs. In all cases, the F···F BCPs have ρ_{BCP} around 10^{-3} a.u. and ∇^2 around 10^{-2} a.u. Therefore, the AIM analysis done on the symmetry unique dimers of C_2F_4 has shown not only the presence of more than one intermolecular C–F···F bond in some dimers but also the simultaneous existence of a C–F···π bond in others.

The biggest perfluorohydrocarbon crystal studied in this work was hexafluorobenzene, C_6F_6, whose crystal Ref. [23] is HFBENZ (see Fig. 1). In this molecule, each F atom is bonded to an aromatic C(sp^2) atom. Consequently, this crystal is helpful to study the impact of carbon aromaticity on the strength of the C(sp^2)–F···F interactions.

There are eleven symmetry unique dimers in this crystal, whose relative orientation is plotted in Fig. 4. The BSSE-corrected intermolecular energy of these dimers, computed at the MP2/aug-cc-pVDZ level, is collected in Table 5, together with the density and Laplacian at the BCP for each of the F···F BCPs found in the analysis of the MP2/aug-cc-pVDZ electron density.

All dimers are energetically stable, but their energy varies widely within the −0.4 to −2.6 kcal/mol range. The weakest energy is found in dimers A and K, where only one F···F intermolecular bond is present and no other intermolecular bond exists. Dimer J, which also has only one F···F bond, presents a F···C (3,−1) bond critical point, indicative of the existence of a C–F···π intermolecular bond (see Fig. S3). Consequently, one can only take the interaction energy in dimers A and K (−0.41 kcal/mol) as a good estimate of the C–F···F bond strength in aromatic carbons. Note that their strength is slightly higher than that

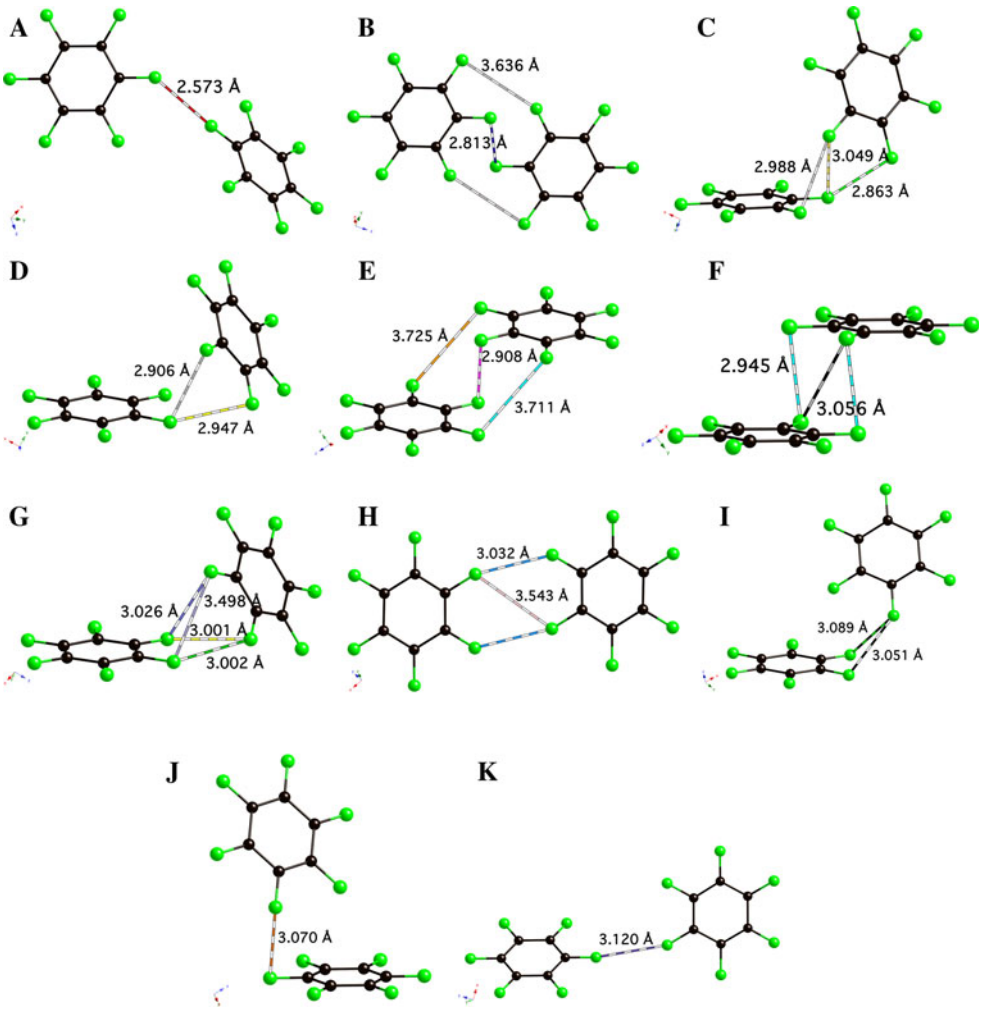

Fig. 4 Geometry of the eleven symmetry non-equivalent dimers found in the C_6F_6 crystal (Ref. [23] HFBENZ). The *broken lines* mark the F atoms involved in C–F···F intermolecular bonds

in non-aromatic C(sp^2)–F···F interactions (−0.25 kcal/mol, measured in dimer C of the C_2F_2 crystal).

All remaining dimers present two (case of dimers B, D, F, H and I), three (dimers C and E) and even four (dimer G) F···F (3,−1) bond critical points. Besides, in dimers D, F and, as already mentioned, J, present a F···C (3,−1) bond critical point indicative of the presence of a C–F···π intermolecular bond (Fig. S2). It is also worth pointing that dimers having the same number and type of intermolecular bonds do not present necessarily similar interaction energies. For instance, dimers C and E have three C–F···F and no other type of intermolecular bond, but the interaction energies are −1.42 and −2.65 kcal/mol. While the interaction energy in dimer C is about three times that of an isolated C–F···F bond in dimer K (−0.41 kcal/mol), which in dimer E is more than six times stronger. These results suggest that the relative orientation of the two interacting molecules is an important factor in determining the strength of C–F···F interactions (more detailed studies described below will confirm the validity of this statement).

Once all C–F···F bond critical points for all three crystals have been determined, one can also evaluate whether their characteristic values follow the general trends previously found for other weak interactions. Particularly, we are interested in testing whether an exponential correlation is found between bond length and the density at the critical point, as was previously found in hydrogen bonds [24, 25]. Figure 5 shows the relationship between the density at the C–F···F bond critical point and the F···F bond length for all F···F bond critical points studied in this work. The points in Fig. 5 follow an exponential dependence between the two variables, similar to that reported on hydrogen bonds [24, 25].

Summarizing the results of the CF_4, C_2F_4 and C_6F_6 crystals, by combining a MP2/aug-cc-pVDZ evaluation of the interaction energy and a AIM search of the intermolecular bonds, it has have been shown that all dimers found in these crystals are energetically stable. The strength of one C–F···F intermolecular bonds was also determined in solid grounds and ranges from −0.21 kcal/mol in dimer B

Table 5 BSSE-corrected intermolecular interaction energy, calculated at MP2/aug-cc-pVDZ level, for the eleven symmetry non-equivalent dimers of C_6F_6 crystal (see Fig. 4)

Dimer	F···F/Å	ΔE/kcal/mol	ρ_{BCP}/a.u.	∇^2_{BCP}/a.u.
A	2.753	−0.45	7.03×10^{-3}	3.92×10^{-2}
B	2.813	−2.59	7.93×10^{-3}	4.68×10^{-2}
	3.636		7.28×10^{-4}	5.99×10^{-3}
C	2.863	−1.42	5.94×10^{-3}	3.42×10^{-2}
	2.988		4.10×10^{-3}	2.76×10^{-2}
	3.049		4.01×10^{-3}	2.66×10^{-2}
D	2.906	−2.16	5.91×10^{-3}	3.41×10^{-2}
	2.947		4.80×10^{-3}	3.01×10^{-2}
E	2.908	−2.65	6.08×10^{-3}	3.85×10^{-2}
	3.711		5.81×10^{-4}	4.77×10^{-3}
	3.725		5.67×10^{-4}	4.63×10^{-3}
F	2.945	−2.64	5.35×10^{-3}	3.28×10^{-2}
	3.056		4.13×10^{-3}	2.82×10^{-2}
G	3.001	−1.81	4.54×10^{-3}	2.98×10^{-2}
	3.002		4.15×10^{-3}	2.58×10^{-2}
	3.026		4.41×10^{-3}	2.92×10^{-2}
	3.498		1.08×10^{-3}	9.13×10^{-3}
H	3.032	−0.62	3.36×10^{-3}	2.20×10^{-2}
	3.543		9.99×10^{-4}	7.81×10^{-3}
I	3.051	−1.98	3.62×10^{-3}	2.36×10^{-2}
	3.089		3.49×10^{-3}	2.33×10^{-2}
J	3.070	−2.57	3.68×10^{-3}	2.48×10^{-2}
K	3.120	−0.41	2.33×10^{-3}	1.69×10^{-2}

For each dimer, its intermolecular F···F bonds are characterized, each one identified by the presence of a (3,−1) bond critical point, whose density (ρ_{BCP}) and Laplacian ($\nabla\rho^2_{BCP}$) at the BCP point are also given. The atoms linked by these F···F bonds are shown in Fig. 4

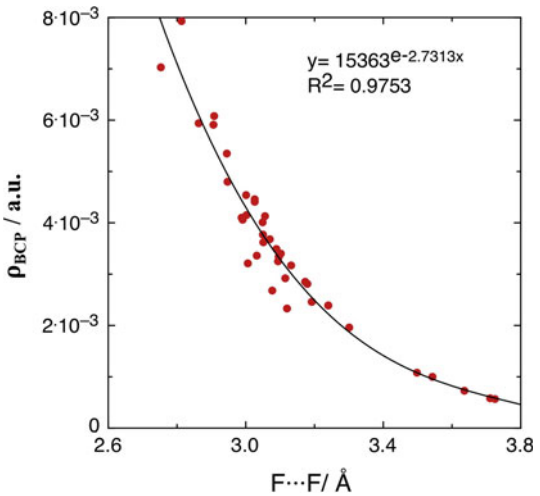

Fig. 5 Variation in the density at the C–F···F bond critical point and the F···F bond length for all F···F bond critical points studied in this work (see Tables 3, 4, 5). The points can be fitted by an exponential equation (see *inset*) with a R^2 regression coefficient of 0.9753

of the CF_4 crystal to −0.41 kcal/mol in dimer K of the C_6F_6 crystal. The hybridization of the carbon atom of the C–F group affects slightly the strength of a single C–F···F bond: −0.21 kcal/mol in C(sp^3), −0.25 kcal/mol in C(non-aromatic sp^2), being more relevant the effect of carbon aromaticity, −0.41 kcal/mol in C(aromatic sp^2). However, the interaction energy of the dimers can be many times stronger due to the presence of multiple C–F···F bonds and of C–F···π bonds. The interaction energy of the dimer grows almost linearly with the number of C–F···F bonds. In some dimers, also C–F···π bonds are present. Dimers with the same number of C–F···F bonds and no C–F···π bonds differ in their interaction, a fact that suggests that the relative orientation of the molecules participating in the C–F···F bond affects the bond strength.

3.3 Relevance of fluorination degree of the hydrocarbon on the C–F···F strength

Perfluorinated C–F···F interactions are not the only type of C–F···F interactions found in crystals. For instance, some crystals present fully F-substituted methyl groups, or even lower substitutions. This fact prompted us to study the impact on the C–F···F interactions of lowering the number of F atoms on CF_4, thus forming CHF_3, CH_2F_2 and CH_3F. This is the simplest model to study C–F···F interactions between dimers of partially fluorinated C atoms.

The impact of fluorination degree on the strength of C–F···F intermolecular interactions could be measured by comparing the strength of dimer B in the CF_4 crystal, and an equivalent dimer taken from the CHF_3, CH_2F_2 and CH_3F crystals. However, this crystal-based approach is not practical: even if crystal structures were available for the CHF_3, CH_2F_2 and CH_3F crystals, very unlikely they will present a dimer B in their packing (the packing of the H-substituted crystals will be dominated by C–H···F bonds). Furthermore, even if they presented a dimer B in their packing, very unlikely it will have the same geometry for the C–F···F contact found in CF_4. Consequently, any direct comparison of the strengths of C–F···F using dimers extracted from crystals will be unreliable, given the different geometries of the C–F···F interactions.

A proper form of comparing the strength of the C–F···F interactions in CF_4, CHF_3, CH_2F_2 and CH_3F dimers is by placing them at the same orientations of the groups involved in the C–F···F contact, whereby allowing the geometry of the two fragments to fully relax at each orientation. Two orientations of the C–F···F contact were initially selected for their study, which can be identified by looking at the two C–F···F angles that one can define in the dimer: (a) the (180,180) or collinear orientation, shown in Fig. 6 and in Fig. 7 insert, and (b) the (90,90) orientation, obtained from the collinear position by changing the two

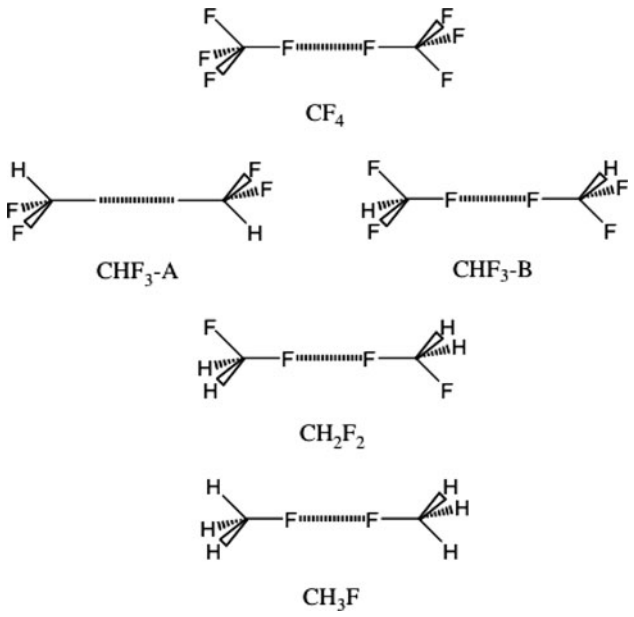

Fig. 6 Relative orientation of the two fragments in the CF_4, CHF_3, CH_2F_2 and CH_3F dimers placed in a (180,180) conformation. The two fragments are in staggered conformation. Two possibilities were distinguished in the CHF_3 dimer, as they give rise to two different orientations when the two C–F···F angles are 90°

C–F···F angles to 90°, shown also in Fig. 7 insert. They are two of the most likely orientations of C–F···F contacts in crystals [7–10]. Note the staggered disposition of the methyl groups in the (180,180) conformation. Also note that, by construction, the two C–F···F angles are always in the same plane.

Figure 7 shows the variation of the interaction energy of the CF_4, CHF_3, CH_2F_2 and CH_3F dimers as a function of the F···F distance of the two atoms linked by broken lines for the (180,180) and (90,90) orientations. The interaction energy and F···F distance at the minimum of each curve are collected in Table 6. Each point of these curves was computed at the MP2/aug-cc-pVDZ, forcing the F···F distance and orientation of the dimer and optimizing the remaining geometrical parameters for all atoms of the dimer.

A proper analysis of Fig. 7 and Table 6 results is only possible once all the intermolecular bonds present in these dimers have been determined. Therefore, in all dimers we systematically searched for their intermolecular bond critical points. At their (180,180) conformation, all dimers present only one F···F bond critical point for the shortest distance F···F distance. However, as shown in Fig. 8, at their (90,90) conformation the situation is more complex: the CF_4 and CHF_3-B dimers present five C–F···F bonds, CHF_3-A just three, and CH_2F_2 and CH_3F only one. No C–H···H or C–H···F bonds were found. Except in the later two cases, no straight forward correlation can be made between dimer strength and C–F···F strength, a fact that makes difficult to look for the angular dependence of C–F···F interactions based only on these two conformations.

The analysis of Figs. 7 and 8 and Table 6 shows some very interesting trends. First of all, in all dimers the (90,90) orientation is more stable than the (180,180) orientation. In CF_4, CHF_3-A and CHF_3-B dimers, this fact is just a consequence of the larger number of C–F···F bonds. In the CH_2F_2 and CH_3F dimers, this higher stability confirms the already indicated angular dependence of the C–F···F interaction. The relative stability of these dimers changes with their orientation. For the (90,90) conformer, the C–F···F interaction energy follows an order $E(CH_2F_2) < E(CH_3F) \approx E(CHF_3\text{-A}) < CF_4 < E(CHF_3\text{-B}) < 0$, being the strongest interaction about −1.8 kcal/mol, value that can be compared with that computed previously of the nearly collinear dimer B of the CF_4 crystal (about −0.2 kcal/mol). However, for the (180,180) conformer $E(CF_4) \approx E(CHF_3) < E(CH_2F_2\text{-A}) = E(CH_2F_2\text{-B}) < 0 < E(CH_3F)$, being the strongest interaction about −0.3 kcal/mol. It is also worth noting the repulsive character of the $CH_3F{\cdots}CH_3F$ interaction in the (180,180) conformation.

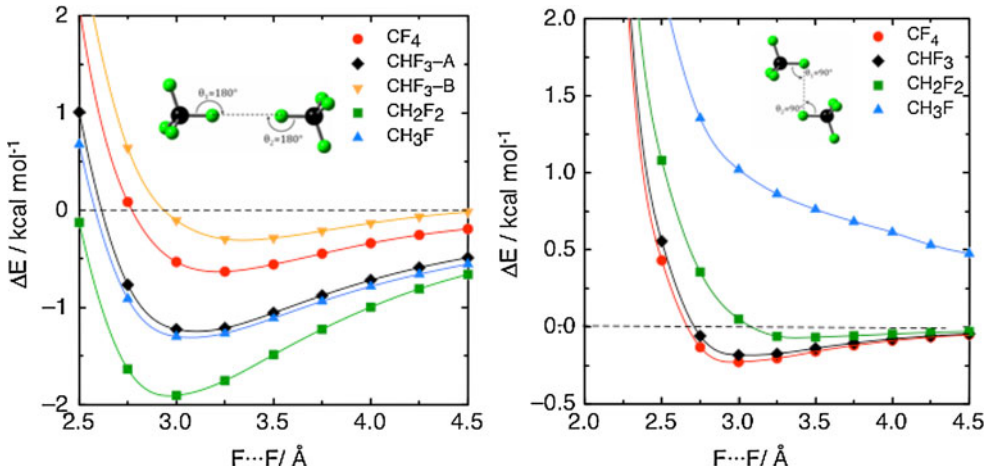

Fig. 7 Potential energy curves for the CF_4, CHF_3, CH_2F_2 and CH_3F dimers. *Left* (180,180) orientation, *right* (90,90) orientation

Table 6 BSSE-corrected intermolecular interaction energy (in kcal/mol) computed at the MP2/aug-cc-pVDZ level for the CF_4, CHF_3, CH_2F_2 and CH_3F dimers at the minimum of potential energy curves of Fig. 7

	F···F/Å	E_{el}	E_{ex}	E_{ind}	E_{disp}	E_{tot}	E_{MP2}
(90,90)							
CF_4	3.25	−0.90	2.35	−0.09	−1.81	−0.45	−0.63
CHF_3-A	3.00	−1.38	1.48	−0.15	−1.25	−1.30	−1.23
CHF_3-B	3.25	0.09	0.40	−0.03	−0.78	−0.32	−0.30
CH_2F_2	3.00	−2.03	1.31	−0.22	−1.04	−1.98	−1.91
CH_3F	3.00	−1.41	1.51	−0.26	−1.19	−1.34	−1.30
(180,180)							
CF_4	3.00	−0.09	0.44	−0.04	−0.48	−0.17	−0.23
CHF_3	3.00	−0.09	0.44	−0.04	−0.48	−0.17	−0.18
CH_2F_2	3.50	0.06	0.02	−0.02	−0.15	−0.08	−0.07
CH_3F	3.00[a]	1.07	0.13	−0.08	−0.27	0.86	0.86

The energy components of the interaction energy calculated using the SAPT method (E_{el}, E_{ex}, E_{ind} and E_{disp}, respectively, the electrostatic, exchange, induction and dispersion components) are also included, together with their sum (E_{tot})

[a] The distance was frozen at this value, because if allowed to be optimized the dimer dissociates

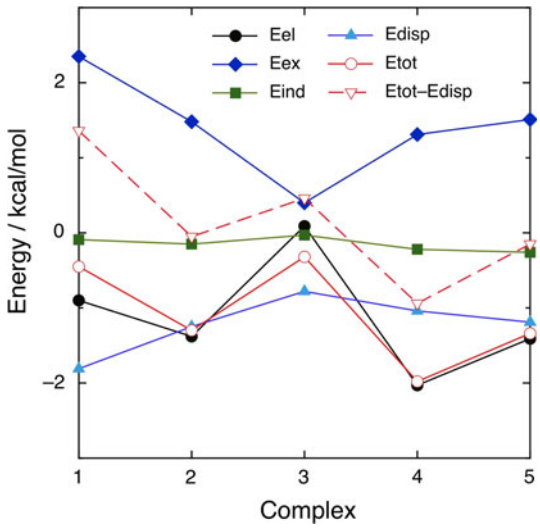

Fig. 9 Variation in the E_{el}, E_{ex}, E_{ind} and E_{disp} energy components (see text for their definition) and their sum (E_{tot}) for the five dimers of Table 6 in their (90,90) conformation. In order to visualize the impact of E_{disp} in E_{tot}, the $E_{tot} - E_{disp}$ variation is also plotted

3.4 The nature of C–F···F interactions

In order to fully understand the trends reported in the previous sections, one needs a proper understanding of the nature of the C–F···F intermolecular interactions. Such understanding can be obtained by evaluating the components of the interaction energy of these dimers, using the SAPT method.

The values of the energy components for all dimers and at the two orientations previously studied are collected in Table 6. It is worth remarking the similarity between the sum of all energy components (E_{tot}) and the BSSE-corrected MP2 interaction energy: these two properties always differ by less than 0.15 kcal/mol and share always the same sign. This is a numerical demonstration of the validity of the SAPT analysis in these dimers. In all dimers, the exchange component (E_{ex}) is always repulsive, while the dispersion (E_{disp}) and induction (E_{ind}) components are always attractive. Finally, the electrostatic component (E_{el}) can be attractive or repulsive, depending on the dimer (in CHF_3, also depends on the relative position of the F and H atoms).

Against the generally accepted idea that F···F interactions are essentially dispersive, Table 6 shows that the dispersion component is not always the dominant one. In various cases (for the (90,90) orientation: all dimers except the CF_4 and CHF_3-B dimers; for the (180,180) orientation: only in the CH_3F dimer), *the electrostatic component is similar or dominates over the dispersion component. Therefore, C–F···F intermolecular interactions have to be considered as having a combined dispersion-electrostatic nature* (based on the two dominant attractive components). The key paper played by the electrostatic and dispersion components is graphically illustrated in Fig. 9, where the values of the E_{el}, E_{ex}, E_{ind}, E_{disp} and E_{tot} for the (90,90) conformation of all Table dimers 6 are plotted (it is worth mentioning that a similar trend is manifested by plotting the components for the (180,180) conformation, although the later figure is not shown here). It is clear from Fig. 9 that E_{ind} always makes a negligible impact on E_{tot}. It is also clear that E_{tot} and E_{el} are nearly on top of each other, the reason being that $E_{disp} \approx -E_{ex}$ in all these dimers. Notice

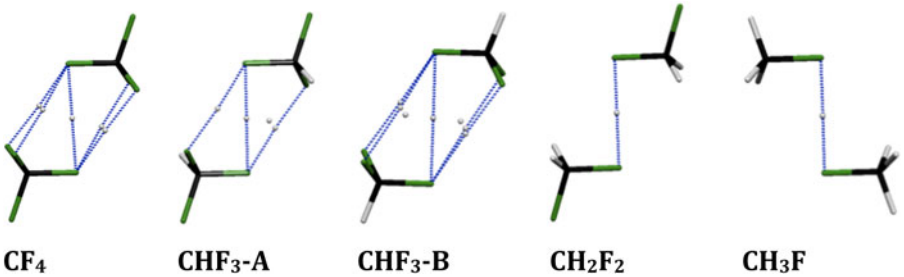

Fig. 8 Intermolecular bond critical points (*white points*) among the fragments of the CF_4, CHF_3, CH_2F_2 and CH_3F dimers, computed at the minimum of their F···F potential energy curves (Fig. 7). The linked points represent bond critical points and the unlinked points are ring or cage points

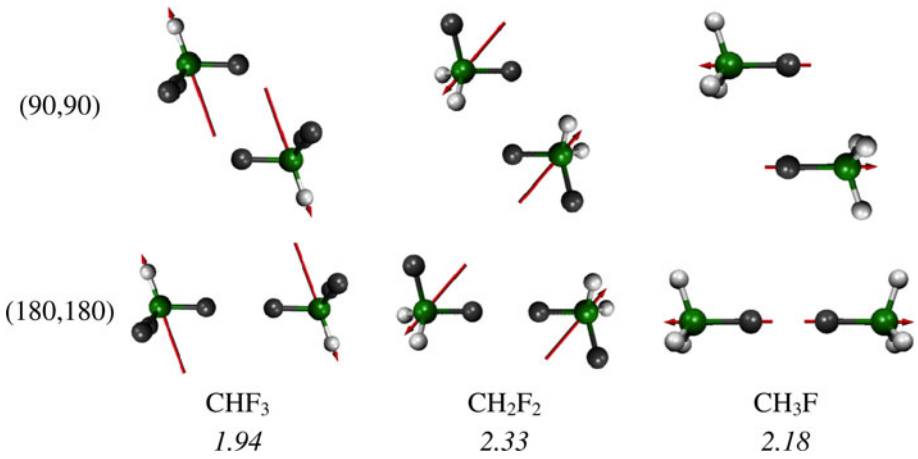

Fig. 10 Relative orientation of the dipole moment in each molecule for the CHF_3, CH_2F_2 and CH_3F dimers. The strength of each dipole moment is also indicated, under the name

also the key paper played by E_{disp}, in the stability of these dimers, clearly manifested by comparing the value of E_{tot} and $E_{tot} - E_{disp}$; while all dimers are stable when E_{disp} is added, all but one are repulsive if such component is deleted.

Once the nature of C–F···F interactions has been determined, it is possible to explain the pending unknowns, using a proper qualitative model for the dispersion and electrostatic energy components. Dispersion can be mostly attributed to the lone–pair···lone–pair interaction generated between the three lone pairs that sit on each of the two F atoms participating in each C–F···F interaction. Accepting that the z-axis lies along the C–F bond, the electronic configuration of the three lone pairs placed on the F atoms can be written as $sp_z^2\ p_x^2\ p_y^2$. Alternatively, it could also be written as $(sp^3)_1^2\ (sp^3)_2^2\ (sp^3)_2^2$. In the first approximation, one expects that the electron density on the F atom is cylindrical but changes with the C–F···F angle (when C–F···F = 180° one hits the sp_z lone pair, while at 90° one hits the p_x or p_y lone pair). In the second case, the electron density on the F atom is nearly spherical in the direction of the lone pairs. The dispersion component in both cases should satisfy the same space symmetry. Therefore, in a first approximation, the density and dispersion for the $sp_z^2\ p_x^2\ p_y^2$ electronic configuration in the (90,90) and (180,180) conformations should differ: in the former case, the lone pairs interacting are the $p_x \cdots p_x$ or $p_y \cdots p_y$, while the later case the interacting lone pairs are the $sp_z \cdots sp_z$. This is contrary to the predictions for the $(sp^3)_1^2\ (sp^3)_2^2\ (sp^3)_2^2$ electron configuration, but in agreement with Table 6 results, and also with results previously reported for Cl···Cl interactions [26]. Note, however, that not all trends in the dispersion component can be explained using this qualitative model. Such qualitative model also predicts that C–F···F interactions in the CHF_3-A and CHF_3-B dimers should be identical, in contradiction to Table 6 results. Therefore, the previous qualitative model is too simplified, because the density of the F atom also depends of the other atoms bonded to the C atom.

According to the electrostatic expansion [27], the most relevant term in the electrostatic component of a neutral molecule is the dipole–dipole term, which depends on the strength and relative orientation of the interacting dipole moments. The MP2/aug-cc-pVDZ dipole moment of the isolated molecules that make the dimers of Table 6, at their isolated optimum geometry, is the following: CF_4: 0 D, CHF_3: 1.94 D, CH_2F_2: 2.33 D and CH_3F: 2.18 D, that is, generally increases with the number of H atoms in the molecule, with the exception of CH_2F_2, which is the biggest one. Such order is that also followed by the electrostatic component. Note, however, that the relevant dipole here is the dipole moment of the isolated molecules *at the geometry that they have at the dimer*. This is clearly demonstrated by looking at the electrostatic component of the (90,90) conformer of the CF_4 dimer, which should be negligible if the two fragments would be at their optimum geometries (because at the optimum geometry their dipole is zero). Finally, the orientation between the two dipoles is also a key property in determining the strength of the electrostatic component, as is demonstrated by looking at the electrostatic component in the CHF_3-A and CHF_3-B dimers.

Other trends can also be explained by looking at the relative orientation of interacting dipoles (Fig. 10). For instance, it is the main factor responsible for the smaller size of the electrostatic component in the (180,180) conformers compared with the (90,90) conformers. It is also the main factor behind the electrostatic component being strongly repulsive in collinear CH_3F dimers (the two dipoles are collinear and point against each other) and weakly attractive or repulsive in all other collinear dimers (antiparallel non-collinear dipoles in CH_2F_2 and CHF_3 dimers; a small dipole induced by small geometrical distortion from a tetrahedral symmetry upon dimer formation, in the CF_4 dimers).

Summarizing the results obtained in the last two sections, C–F···F interactions have a combined dispersion-electrostatic

nature, where in many cases both components have similar weight. In collinear orientations, the strength of C–F···F interactions becomes weaker as the H-substitution increases, being repulsive at the maximum substitution, CH_3F. The sign and the strength of the electrostatic component can be rationalized by looking at the size and orientation of the dipole moments located in each of the molecules of the dimer. This makes the strength of the dimer interaction energy strongly dependent on the degree of F-substitution and the two C–F···F angles.

4 Conclusions

The nature, strength and directionality of the C–F···F intermolecular interactions present in crystals of fully and partly fluorinated hydrocarbons have been theoretically evaluated. The study was done in three consecutive steps: (1) evaluation of the MP2/aug-cc-pVDZ interaction energy, (2) determination of all F···F bond critical points and (3) SAPT analysis of the energy components of the dimers. The study was done for all symmetry unique dimers present in the CF_4, C_2F_4 and C_6F_6 crystals and for CF_4, CHF_3, CH_2F_2 and CH_3F model dimers placed in a (180,180) and a (90,90) conformation.

We can conclude that all dimers found in the CF_4, C_2F_4 and C_6F_6 crystals are energetically stable and their strength varying from −0.21 kcal/mol (in dimer B of the CF_4,) to −2.65 kcal/mol (in dimer E, C_6F_6 crystal). However, as more than one C–F···F bond is sometimes present in these dimers, and even C–F···π bonds are sometimes found, one cannot equate the dimer stability to the strength of a single C–F···F interaction. By selecting dimers presenting a single C–F···F bond (as indicated by doing locating F···F (3,−1) bond critical points in a AIM analysis), one can assign the following values to the strength of a single C–F···F bond: −0.21 kcal/mol in C(sp^3) atoms, −0.25 kcal/mol in C(non-aromatic sp^2), −0.41 kcal/mol in C(non-aromatic sp^2). The interaction energy of the dimer grows almost linearly with the number of C–F···F bonds present (the lack of linearity can be attributed to angular dependencies and possible cooperative effects). The relative orientation of the C–F···F bond affects its strength. SAPT calculations indicate that in collinear CF_4 dimers, C–F···F interactions are strongly dominated by the dispersion energetic component, while when in the (90,90) conformation the electrostatic component becomes also important dispersion.

The strength, angular dependence and nature of the C–F···F interactions found in the CHF_3, CH_2F_2 and CH_3F model dimers change relative to that found in CF_4 dimers placed at the same orientation. In a collinear, or (180,180), orientation, the strength of C–F···F interactions becomes weaker as more H atoms are bonded to the carbon atoms, being repulsive at the maximum substitution, CH_3F. In a (90,90) orientation, the strength can be weaker or stronger depending on the dipole moment orientation, being the strongest interaction −2.0 kcal/mol (in CF_4 dimers is −0.45 kcal/mol). The nature becomes a combined dispersion plus electrostatic components, in many cases, both components having a similar weight.

Acknowledgments The Barcelona team thanks support by MICINN, the Spanish Science and Innovation Ministry (MAT2008-02032/MAT and UNBA05-33-001 and postdoctoral contract to ED) and the CIRIT (2009 SGR 1203). CESCA and BSC computer time is also acknowledged. The Malaga team thanks support by MICINN (project CTQ2009–10098) and Junta de Andalucia (grant FQM-0159 and project P06-FQM-1678). R. M. O. is also grateful to the MICINN for her Ph.D. Grant, and the UMA and BSC for mobility grants that made possible her stay at UB during her Ph. D.

References

1. Sakamoto Y, Suzuki T, Kobayashi M, Gao Y, Fukai Y, Inoue Y, Sato F, Tokito S (2004) Perfluoropentacene: high-performance p-n junctions and complementary circuits with pentacene. J Am Chem Soc 126:8138–8140
2. Schön JH, Kloc Ch, Batlogg B (2000) Fractional quantum hall effect in organic molecular semiconductors. Science 288:2338–2340
3. Siegrist T, Kloc C, Schön JH, Batlogg B, Haddon RC, Berg S, Thomas GA (2001) Enhanced physical properties in a pentacene polymorph. Angew Chem Int Ed 40:1731–1736
4. Heidenhain SB, Sakamoto Y, Suzuki T, Miura A, Fujikawa H, Mori T, Tokito S, Taga Y (2000) Perfluorinated oligo(p-phenylene)s: efficient n-type semiconductors for organic light-emitting diodes. J Am Chem Soc 122:10240–10241
5. Ruiz Delgado MC, Pigg KR, da Silva Filho DA, Gruhn NE, Sakamoto Y, Suzuki T, Malave Osuna R, Casado J, Hernandez V, Lopez Navarrete JT, Martinelli NG, Cornil J, Sanchez-Carrera RS, Coropceanu V, Bredas J-L (2009) Impact of perfluorination on the charge-transport parameters of oligoacene crystals. J Am Chem Soc 131:1502–1512
6. Lentz D, Bach A, Buschmann J, Luger P, Messerschmidt M (2004) Crystal and molecular structures and experimentally determined charge densities of fluorinated ethenes. Chem Eur J 10:5059–5066
7. Reichenbächer K, Süss HI, Hulliger J (2005) Fluorine in crystal engineering—the little atom that could. Chem Soc Rev 34:22–30
8. Desiraju GR, Parthasarathy R (1989) The nature of halogen···halogen interactions: are short halogen contacts due to specific attractive forces or due to close packing of nonspherical atoms? J Am Chem Soc 111:8725–8726
9. Choudhury AR, Row TNG (2006) Organic fluorine as crystal engineering tool: evidence from packing features in fluorine substituted isoquinolines. CrystEngComm 8:265–274
10. Prasanna MD, Guru Row TN (2001) Weak interactions involving organic fluorine: analysis of structural motifs in Flunazirine and Haloperidol. J Mol Struct 562:55–61
11. Alkorta I, Elguero J (2004) Fluorine–fluorine interactions: NMR and AIM analysis. Struct Chem 15:117–120
12. Bader RFW (1994) Atoms in molecules: a quantum theory. Oxford University Press, New York
13. D'Oria E, Novoa JJ (2008) On the hydrogen bond nature of the C–HF interactions in molecular crystals. An exhaustive

investigation combining a crystallographic database search and ab initio theoretical calculations. CrystEngComm 10:423–436
14. Choudhury AR, Row TNG (2006) Organic fluorine as crystal engineering tool: evidence from packing features in fluorine substituted isoquinolines. CrystEngComm 8:265–274
15. Frisch MJ, Trucks GW, Schlegel HB, Scuseria GE, Robb MA, Cheeseman JR, Montgomery JA, Vreven T, Kudin KN, Burant JC, Millam JM, Iyengar SS, Tomasi J, Barone V, Mennucci B, Cossi M, Scalmani G, Rega N, Petersson GA, Nakatsuji H, Hada M, Ehara M, Toyota K, Fukuda R, Hasegawa J, Ishida M, Nakajima T, Honda Y, Kitao O, Nakai H, Klene M, Li X, Knox JE, Hratchian HP, Cross JB, Adamo C, Jaramillo J, Gomperts R, Stratmann RE, Yazyev O, Austin AJ, Cammi R, Pomelli C, Ochterski JW, Ayala PY, Morokuma K, Voth GA, Salvador P, Dannenberg JJ, Zakrzewski VG, Dapprich S, Daniels AD, Strain MC, Farkas O, Malick DK, Rabuck AD, Raghavachari K, Foresman JB, Ortiz JV, Cui Q, Baboul G, Clifford S, Cioslowski J, Stefanov BB, Liu G, Liashenko A, Piskorz P, Komaromi IA, Martin RL, Fox DJ, Keith T, Al-Laham MA, Peng CY, Nanayakkara A, Challacombe M, Gill PMW, Johnson B, Chen W, Wong MW, Gonzalez C, Pople JA (2004) Gaussian 03, revision E.01. Gaussian, Inc., Wallingford
16. Boys SF, Bernardi F (1970) Calculation of small molecular interactions by differences of separate total energies. Some procedures with reduced errors. Mol Phys 19:553–566
17. van Duijneveldt FB, van Duijneveldt-van de Rijdt JGCM, van Lenthe JH (1994) State-of-the-art in counterpoise theory. Chem Rev 94:1873–1885
18. Novoa JJ, Planas M, Whangbo MH (1994) A numerical evaluation of the counterpoise method on hydrogen-bond complexes using near complete basis-sets. Chem Phys Let 225:240–246
19. Woon DE, Dunning TH (1993) Gaussian-basis sets for use in correlated molecular calculations. 3. The atoms aluminum through argon. J Chem Phys 98:1358–1371
20. Biegler-Konig FW, Bader RFW, Tang TH (1982) Calculation of the average properties of atom in molecules. 2. J Comput Chem 3:317–328
21. Jeziorski B, Moszynski R, Szalewicz K (1994) Perturbation theory approach to intermolecular potential energy surfaces of van der Waals complexes. Chem Rev 94:1887–1930
22. Bukowski R, Cencek W, Jankowski P, Jeziorski B, Jeziorska M, Kucharski SA, Lotrich VF, Misquitta AJ, Moszynski R, Patkowski K, Podeszwa R, Rybak S, Szalewicz K, Williams HL, Wheatley RJ, Wormer PES, Żuchowski PS (1994) SAPT2008: an ab initio program for many-body symmetry-adapted perturbation theory calculations of intermolecular interaction energies. Chem Rev 94:1887–1930
23. Allen FH (2002) The Cambridge structural database: a quarter of a million crystal structures and rising. Acta Cryst B 58:380–388
24. Espinosa E, Molins E, Lecomte C (1998) Hydrogen bond strengths revealed by topological analyses of experimentally observed electron densities. Chem Phys Lett 285:170–173
25. Mata I, Alkorta I, Molins E, Espinosa E (2010) Universal features of the electron density distribution in hydrogen-bonding regions: a comprehensive study involving H center dot center dot center dot X (X = H, C, N, O, F, S, Cl, pi) interactions. Chem Eur J 16:2442–2452
26. Price SL, Stone AJ (1982) The anisotropy of the Cl-Cl pair potential as shown by the crystal-structure—evidence for intermolecular bonding or lone pair effects. Mol Phys 47:1457–1470
27. Stone AJ (1996) The theory of intermolecular forces. Clarendon Press, Oxford